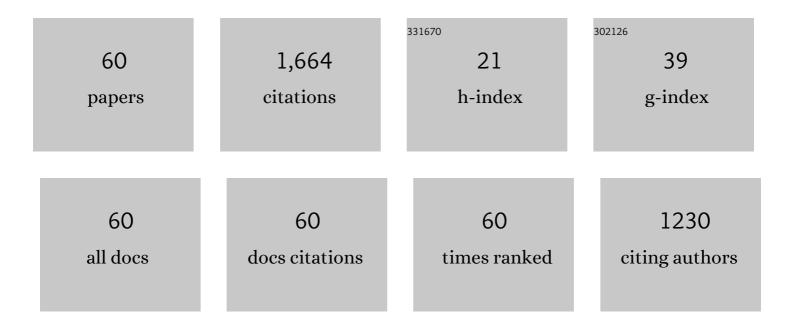
Chih-Kuang Lin

List of Publications by Year in descending order

Source: https://exaly.com/author-pdf/7514130/publications.pdf Version: 2024-02-01



Снин-Килло Цил

#	Article	IF	CITATIONS
1	Thermal stress analysis of a planar SOFC stack. Journal of Power Sources, 2007, 164, 238-251.	7.8	232
2	Effect of trace La addition on the microstructures and mechanical properties of A356 (Al–7Si–0.35Mg) aluminum alloys. Journal of Alloys and Compounds, 2009, 487, 157-162.	5.5	174
3	Thermal stress analysis of planar solid oxide fuel cell stacks: Effects of sealing design. Journal of Power Sources, 2009, 192, 515-524.	7.8	99
4	Tensile and fatigue properties of 17-4 PH stainless steel at high temperatures. Metallurgical and Materials Transactions A: Physical Metallurgy and Materials Science, 2002, 33, 1715-1724.	2.2	64
5	Effects of Nb and W additions on high-temperature creep properties of ferritic stainless steels for solid oxide fuel cell interconnect. Journal of Power Sources, 2012, 198, 149-157.	7.8	64
6	Effects of crystallization on the high-temperature mechanical properties of a glass sealant for solid oxide fuel cell. Journal of Power Sources, 2010, 195, 3159-3165.	7.8	61
7	Title is missing!. Journal of Materials Science, 2003, 38, 965-971.	3.7	58
8	Effect of trace Ce addition on the microstructures and mechanical properties of A356 (AL–7SI–0.35 Mg) aluminum alloys. Journal of the Chinese Institute of Engineers, Transactions of the Chinese Institute of Engineers,Series A/Chung-kuo Kung Ch'eng Hsuch K'an, 2011, 34, 609-616.	1.1	58
9	High-temperature tensile and creep properties of a ferritic stainless steel for interconnect in solid oxide fuel cell. Journal of Power Sources, 2011, 196, 2005-2012.	7.8	56
10	High-temperature mechanical properties of a glass sealant for solid oxide fuel cell. Journal of Power Sources, 2009, 189, 1093-1099.	7.8	46
11	Effect of strain rate on high-temperature low-cycle fatigue of 17-4 PH stainless steels. Materials Science & Engineering A: Structural Materials: Properties, Microstructure and Processing, 2005, 390, 291-298.	5.6	40
12	Joint strength of a solid oxide fuel cell glass–ceramic sealant with metallic interconnect. Journal of Power Sources, 2012, 205, 307-317.	7.8	39
13	Conductive Characteristics of Indium Tin Oxide Thin Film on Polymeric Substrate under Long-Term Static Deformation. Coatings, 2018, 8, 212.	2.6	39
14	High-temperature mechanical properties of a solid oxide fuel cell glass sealant in sintered forms. Journal of Power Sources, 2011, 196, 3583-3591.	7.8	36
15	Creep rupture of lead-free Sn-3.5Ag and Sn-3.5Ag-0.5Cu solders. Journal of Materials Science: Materials in Electronics, 2005, 16, 355-365.	2.2	34
16	Effects of cyclic hydriding–dehydriding reactions of Mg2Ni alloy on the expansion deformation of a metal hydride storage vessel. Journal of Alloys and Compounds, 2011, 509, 7162-7167.	5.5	33
17	Effects of cyclic hydriding–dehydriding reactions of LaNi5 on the thin-wall deformation of metal hydride storage vessels with various configurations. Renewable Energy, 2012, 48, 404-410.	8.9	26
18	Joint strength of a solid oxide fuel cell glass–ceramic sealant with metallic interconnect in a reducing environment. Journal of Power Sources, 2015, 280, 272-288.	7.8	25

CHIH-KUANG LIN

#	Article	IF	CITATIONS
19	Mechanical behaviour of a granular solid and its contacting deformable structure under uni-axial compression – Part I: Joint DEM–FEM modelling and experimental validation. Chemical Engineering Science, 2016, 144, 404-420.	3.8	25
20	Aging effects on high-temperature creep properties of a solid oxide fuel cell glass-ceramic sealant. Journal of Power Sources, 2013, 241, 12-19.	7.8	23
21	High-Cycle Fatigue of Austempered Ductile Irons in Various-Sized Y-Block Castings. Materials Transactions, JIM, 1997, 38, 682-691.	0.9	22
22	Dynamic strain aging in low cycle fatigue of duplex titanium alloys. Materials Science & Engineering A: Structural Materials: Properties, Microstructure and Processing, 2011, 528, 4381-4389.	5.6	22
23	Creep rupture of the joint of a solid oxide fuel cell glass–ceramic sealant with metallic interconnect. Journal of Power Sources, 2014, 245, 787-795.	7.8	20
24	Creep rupture of the joint between a glass-ceramic sealant and lanthanum strontium manganite-coated ferritic stainless steel interconnect for solid oxide fuel cells. Journal of the European Ceramic Society, 2018, 38, 2417-2429.	5.7	20
25	Influence of Frequency on High-Temperature Fatigue Behavior of 17-4 PH Stainless Steels. Materials Transactions, 2003, 44, 713-721.	1.2	19
26	High-temperature fatigue crack growth behavior of 17-4 PH stainless steels. Metallurgical and Materials Transactions A: Physical Metallurgy and Materials Science, 2004, 35, 3018-3024.	2.2	19
27	Effects of continuously applied stress on tin whisker growth. Microelectronics Reliability, 2008, 48, 1737-1740.	1.7	19
28	An extreme learning machine for predicting kerf waviness and heat affected zone in pulsed laser cutting of thin non-oriented silicon steel. Optics and Lasers in Engineering, 2020, 134, 106244.	3.8	19
29	Influence of heat treatment on fatigue crack growth of austempered ductile iron. Journal of Materials Science, 2002, 37, 709-716.	3.7	18
30	Effects of Build Direction on the Mechanical Properties of a Martensitic Stainless Steel Fabricated by Selective Laser Melting. Materials, 2020, 13, 5142.	2.9	16
31	Thermo-mechanical fatigue properties of a ferritic stainless steel for solid oxide fuel cell interconnect. Journal of Power Sources, 2012, 219, 112-119.	7.8	15
32	Mechanical durability of solid oxide fuel cell glass-ceramic sealant/steel interconnect joint under thermo-mechanical cycling. Renewable Energy, 2019, 138, 1205-1213.	8.9	15
33	Effects of Laser Spot Size on the Mechanical Properties of AISI 420 Stainless Steel Fabricated by Selective Laser Melting. Materials, 2021, 14, 4593.	2.9	15
34	Prediction and optimization of dross formation in laser cutting of electrical steel sheet in different environments. Journal of Materials Research and Technology, 2022, 18, 1977-1990.	5.8	13
35	Low-Cycle Fatigue of Austempered Ductile Irons in Various-Sized Y-Block Castings. Materials Transactions, JIM, 1997, 38, 692-700.	0.9	12
36	Analysis of structural deformation and deformation-induced solar radiation misalignment in a tracking photovoltaic system. Renewable Energy, 2013, 59, 65-74.	8.9	12

CHIH-KUANG LIN

#	Article	IF	CITATIONS
37	Effects of cyclic deformation on conductive characteristics of indium tin oxide thin film on polyethylene terephthalate substrate. Surface and Coatings Technology, 2015, 283, 298-310.	4.8	12
38	Prediction and optimization of geometrical quality for pulsed laser cutting of non-oriented electrical steel sheet. Optics and Laser Technology, 2022, 149, 107847.	4.6	12
39	An improved real-time temperature control for pulsed laser cutting of non-oriented electrical steel. Optics and Laser Technology, 2021, 136, 106783.	4.6	11
40	Fatigue behavior of AISI 347 stainless steel in various environments. Journal of Materials Science, 2004, 39, 6901-6908.	3.7	10
41	Creep properties of Sn-3.5Ag-0.5Cu lead-free solder under step-loading. Journal of Materials Science: Materials in Electronics, 2006, 17, 577-586.	2.2	10
42	Influence of Frequency on the High-Temperature Fatigue Crack Growth Behavior of 17-4 PH Stainless Steels. Materials Transactions, 2007, 48, 490-499.	1.2	10
43	Artificial intelligence-based modeling and optimization of heat-affected zone and magnetic property in pulsed laser cutting of thin nonoriented silicon steel. International Journal of Advanced Manufacturing Technology, 2021, 113, 3225-3240.	3.0	10
44	Effects of cyclic deformation on a barrier thin film for flexible organic optoelectronic devices. Thin Solid Films, 2018, 650, 20-31.	1.8	9
45	DEM simulation and experimental validation for mechanical response of ellipsoidal particles under confined compression. Advanced Powder Technology, 2018, 29, 1292-1305.	4.1	9
46	Interfacial fracture resistance of the joint of a solid oxide fuel cell glass–ceramic sealant with metallic interconnect. Journal of Power Sources, 2014, 261, 227-237.	7.8	8
47	Effects of R-ratio on high-temperature fatigue crack growth behavior of a precipitation-hardening stainless steel. International Journal of Fatigue, 2008, 30, 2147-2155.	5.7	7
48	Effect of the Spinning Deformation Processing on Mechanical Properties of Al-7Si-0.3Mg Alloys. Journal of Materials Engineering and Performance, 2012, 21, 1873-1878.	2.5	7
49	Corrosion fatigue of austempered ductile iron. Journal of Materials Science, 2003, 38, 1667-1672.	3.7	6
50	Analysis of structural deformation and concentrator misalignment in a roll-tilt solar tracker. , 2013, , .		6
51	Effects of Particle Stiffness on Mechanical Response of Granular Solid Under Confined Compression. Procedia Engineering, 2014, 79, 143-152.	1.2	5
52	A Hybrid PSO–GWO Fuzzy Logic Controller with a New Fuzzy Tuner. International Journal of Fuzzy Systems, 2022, 24, 1586-1604.	4.0	5
53	Controller Design for Unstable Time-Delay Systems with Unknown Transfer Functions. Mathematics, 2022, 10, 431.	2.2	5
54	Effects of Long-Term Static Bending Deformation on a Barrier Thin Film for Flexible Organic Optoelectronic Devices. Coatings, 2018, 8, 127.	2.6	4

CHIH-KUANG LIN

#	Article	IF	CITATIONS
55	Low-cycle fatigue behavior of AISI 347 stainless steel in salt water. Journal of Materials Science, 2007, 42, 40-49.	3.7	3
56	Statistical Analysis of Size Effects on Time-Dependent Fracture of an Alumina. Journal of the Ceramic Society of Japan, 1997, 105, 723-730.	1.3	2
57	Formation of Bottom Conjugate Pair Grooves by Femtosecond Laser Grooving on Transparent Substrate. IEEE Photonics Technology Letters, 2021, 33, 305-308.	2.5	2
58	Design of Optimal Controllers for Unknown Dynamic Systems through the Nelder–Mead Simplex Method. Mathematics, 2021, 9, 2013.	2.2	2
59	Environmental Effects on Fatigue Crack Growth in Austempered Ductile Irons. Materials Transactions, 2001, 42, 1085-1094.	1.2	1
60	Size Effect on Thermal Shock Behavior of an Alumina. Journal of the Ceramic Society of Japan, 1997, 105, 1062-1066.	1.3	0